Title: Revealing fast proton transport in condensed matter by means of density scaling concept

Author: Żaneta Wojnarowska, Małgorzata Musiał, Shinian Cheng, Jacek Gapinski, Adam Patkowski, Jürgen Pionteck, Marian Paluch

Citation style: Wojnarowska Żaneta, Musiał Małgorzata, Cheng Shinian, Gapinski Jacek, Patkowski Adam, Pionteck Jürgen, Paluch Marian. (2020). Revealing fast proton transport in condensed matter by means of density scaling concept. "The Journal of Physical Chemistry C" iss. 29, (2020), s. 15749-15756.
DOI: 10.1021/acs.jpcc.0c03548

THE JOURNAL OF PHYSICAL CHEMISTRY C

pubs.acs.org/JPCC

Article

Revealing Fast Proton Transport in Condensed Matter by Means of Density Scaling Concept

Zaneta Wojnarowska,* Małgorzata Musiał, Shinian Cheng, Jacek Gapinski, Adam Patkowski, Jürgen Pionteck, and Marian Paluch

Cite This: *J. Phys. Chem. C* 2020, 124, 15749−15756

Read Online

ACCESS | Metrics & More | Article Recommendations

ABSTRACT: Herein, we investigate the charge transport and structural dynamics in the supercooled and glassy state of protic ionic material with an efficient interionic Grotthuss mechanism. We found that superprotonic properties of studied acebutolol hydrochloride (ACB-HCl) depend on thermodynamic conditions with the most favorable regions being close to the glass-transition temperature (T_g) and glass-transition pressure (P_g). To quantify the contribution of fast proton hopping to overall charge transport over a broad $T-P$ space, we employed the density scaling concept, one of the most important experimental findings in the field of condensed matter physics. We found that isothermal and isobaric dc-conductivity (σ_{dc}) and dynamic light scattering (τ_α) data of ACB-HCl plotted as a function of $(TV^\gamma)^{-1}$ satisfy the thermodynamic scaling criterion with the ratio $\gamma_\sigma/\gamma_\alpha$ appearing as a new measure of fast charge transport in protic ionic glass-formers in the $T-P$ plane. Such a universal factor becomes an alternative to the well-known Walden rule being limited to ambient pressure conditions.

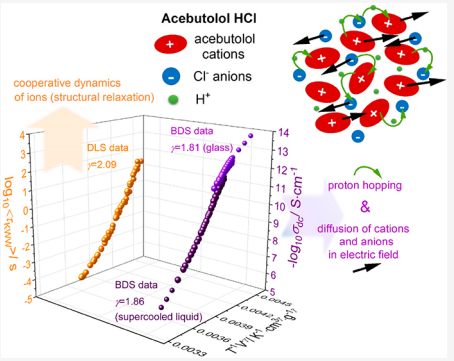

INTRODUCTION

Charge transport through intermolecular proton hopping is considered essential for many chemical processes. In particular, it has been identified as the main mechanism underlying various biological functions and properties of such basic substances like proteins and water.[1−3] Proton transport in condensed matter is, in turn, a fundamental phenomenon across a wide range of technologies and applications.[4] For example, solid-state electrolytes with effective proton conductivity in anhydrous conditions have become a promising alternative for water-saturated fuel cell membranes that are useless above 100 °C.[5]

Continuing the latest strategy, considerable attention of the scientific community has been focused on protic ionic (PI) glass-formers. A vital feature of these materials is their hassle-free transformation to the disordered glassy state by isobaric cooling or isothermal compression. Chemically, they are ion-containing liquids or solids obtained in proton transfer reaction from Bronsted acid (HA) to Bronsted base (B) and characterized by a substantial contribution of H-bonding to intermolecular interactions.[6] Depending on the donor−acceptor capabilities of the parent compounds participating in this process, the neutralization reaction is more or less efficient resulting in fully or partially ionized products. The protic ionic systems composed solely of ions are characterized by charge transport of "vehicle" features, i.e., involving proton migration only via translational diffusion of cations (BH^+).[7] On the other hand, in partially ionized protic glass-formers H^+ motions are additionally accessible through the Grotthuss pathways, i.e., local H^+ migration from one molecule to another by using "highways" made of hydrogen bonds.[8,9] The latter mechanism, which gives a substantial contribution to charge transport, is found to be responsible for superionic properties of various PI glass-formers including phosphoric acid, which is considered to be the best proton conductor.[10] Since fast intermolecular H^+ hopping along the Grotthuss paths is independent of ion diffusion, the basic physical quantities describing the PI system, i.e., molar conductivity (Λ_{mol}) and viscosity (η), become decoupled from each other.

Generally, two methods are providing a quantitative measure of decoupling phenomenon, and thereby proton transport efficiency. The first one is based on the Walden plot: $\log_{10}\Lambda_{mol}$ vs. $\log_{10}\eta^{-k}$. If the experimental data are located in the superionic region of the Walden graph (i.e., above the ideal line determined for diluted KCl), then the lower exponent k indicates the greater decoupling. Note that $k < 1$.[11,12] In an alternative approach, the decoupling index describing the time

Received: April 21, 2020
Revised: June 20, 2020
Published: June 25, 2020

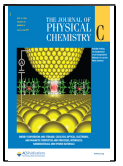

scale separation between structural reorientation ($\tau_\alpha = \eta/G^\infty$) and electrical relaxation ($\tau_\sigma = \varepsilon_0\varepsilon_s M/\rho\Lambda_{mol}$) at the temperature of liquid−glass transition, $R(T_g) = \log_{10}\tau_\alpha(T_g) - \log_{10}\tau_\sigma(T_g)$, is employed.[13] Importantly, the former method quantifies the proton transport over a broad T range while the latter one is limited to a single point, the T_g temperature, i.e., the region where H^+ hopping is the most efficient. Nevertheless, neither of these two procedures can be employed to provide a unified description of proton transport at various temperature and pressure conditions by using a single variable. This is because H^+ transfer becomes faster at elevated pressure, breaking the Walden rule and raising the decoupling index at the glass-transition pressure $R(P_g)$ in comparison to $R(T_g)$.[14,15] Additionally, there is no correlation between the degree of decoupling at ambient conditions and its pressure dependence.[16] In this context, the following question arises: How can we quantify the effectiveness of proton transport over a broad $T-P$ thermodynamic space?

A well-established concept describing the dynamics of ion-containing systems (others as well) at various $T-P$ conditions is based on the density scaling rule. According to this idea, dc-conductivity ($\sigma_{dc} = \Lambda_{mol}\rho/M$), viscosity ($\eta$), structural relaxation time (τ_α), diffusion (D), or any other dynamic quantity recorded over a broad $T-P$ range can be expressed as a universal curve if plotted against TV^γ, where T and V denote temperature and specific volume, respectively, and γ is the scaling exponent.[17] The magnitude of parameter γ is related to the repulsive part of the effective short-range intermolecular potential,[18] and thereby, it is usually associated with the structure of a given material. It is also directly connected to the thermodynamically defined Grüneisen constant (γ_G) and, thus, provides a bridge between the dynamics and thermodynamics.[19]

It has been confirmed multiple times in the literature that the density scaling concept is satisfied for ionic systems regardless of the huge structural diversity of these materials and various types of intermolecular interactions existing between ions (electrostatics, van der Waals, π-stacking of the cation, and H-bonding).[20−22] Importantly, the TV^γ scaling was found to be valid perfectly even when ion dynamics over a wide range of temperature, pressure, and density (ρ changes up to 20%)[23] is considered. Additionally, for aprotic ionic systems, characterized by charge transport fully controlled by ion diffusion (vehicle mechanism), a state-point-independent γ is obtained independently of the dynamic properties being tested.[24] This allows us to believe that the time scale separation existing between charge and mass transport in proton-conducting glass-formers will bring different values of the γ coefficient for $\log_{10}\sigma_{dc} = f(TV^\gamma)$ and $\log_{10}\eta = f(TV^\gamma)$ scaling. If such a scenario comes true, the ratio $\gamma_\sigma/\gamma_\eta$ can be treated as a new measure of Grotthuss conduction in protic ionic materials both at ambient and elevated pressures. The potential effect of H^+ hopping on thermodynamic quantities, including Grüneisen constant γ_G being related to scaling exponent γ, becomes a second unresolved problem.

In this work, we verify the above-mentioned issues by investigating the dynamic and thermodynamic properties of acebutolol hydrochloride (ACB-HCl) at various $T-P$ conditions. There are two reasons to justify the choice of the studied sample. First, this ionic material can be easily transformed into the glassy state (T_g = 315 K) by quenching of the melt (T_m = 417 K). Second, as confirmed by DFT calculations and Brillouin scattering measurements,[25] ACB-HCl is characterized by efficient interionic proton transport supported by intramolecular H^+ hopping. Herein, we investigate the isothermal and isobaric dc-conductivity and structural relaxation behavior of ACB-HCl in terms of the density scaling concept. We found that $\tau_\alpha(T, P)$ and $\sigma_{dc}(T, P)$ dependences, determined from dynamic light scattering−photon correlation spectroscopy (DLS) experiments and broadband dielectric spectroscopy (BDS) measurements, respectively, recalculated to TV^γ representation, both satisfy the scaling law, however with different γ coefficients. Additionally, a further decrease of γ_σ is observed when the liquid−glass transition is passed through. On the other hand, the thermodynamic quantities seem not to be sensitive to fast proton hopping.

EXPERIMENTAL SECTION

Conductivity Measurements. Dielectric experiments of ACB-HCl were performed in the external electric field (0.5 V) with a frequency interval of 10^{-1} to 10^6 Hz and a wide temperature range, covering the supercooled liquid regime as well as the glassy state. Isobaric measurements at ambient pressure were carried out using a ALPHA High Grade Dielectric Analyzer (Novocontrol Technologies GmbH). For the isobaric measurements, the sample was placed between two stainless steel electrodes of the capacitor with a gap of 0.1 mm. The dielectric spectra of ACB-HCl were collected over a wide temperature range from 355 to 173 K. The temperature was controlled by the Novocontrol Quattro system, with the use of a nitrogen gas cryostat. The temperature stability of the system was better than 0.1 K. For the pressure-dependent dielectric measurements, we used a capacitor, filled with the ACB-HCl sample, which was next placed in the high-pressure chamber and compressed using silicone oil. Note that during the measurement the sample was in contact with stainless steel and Teflon. The pressure was controlled with an accuracy of 0.1 MPa. The temperature was controlled within 0.1 K employing a liquid flow provided by a Weiss fridge. The measurements were performed in the following pressure ranges: 20−160 MPa at 323 K; 20−290 MPa at 333 K; 0.1−425 MPa at 343 K; 20−500 MPa at 353 K.

Dynamic Light Scattering (DLS). For details of DLS measurements of ACB-HCl, see ref 26.

PVT. The *PVT* measurements were performed using a high-pressure dilatometer (a fully automated GNOMIX).[27] The details can be found in refs 28 and 29. *PVT* data in the pressure range up to 200 MPa, and from room temperature up to 433 K, were collected in the isobaric standard mode. The values for 0.1 MPa were obtained by extrapolation of the data measured in the range 40−200 MPa in steps of 40 MPa according to the Tait equation. In the studied range, the accuracy limit for the absolute values of the specific volume is within 0.002 $cm^3\ g^{-1}$. Because *PVT* devices measure only the changes in the specific volume, it is necessary to correct the measured values by adding the specific volume under known, typically ambient conditions, which is 0.845 $cm^3\ g^{-1}$ (determined by means of helium pycnometer at 0.1 MPa and 293.15 K).

RESULTS AND DISCUSSION

The conducting properties of ACB-HCl in the supercooled and glassy states were evaluated using ambient and high-pressure dielectric measurements. The representative electric conductivity spectra measured during isobaric cooling and

https://dx.doi.org/10.1021/acs.jpcc.0c03548
J. Phys. Chem. C 2020, 124, 15749−15756

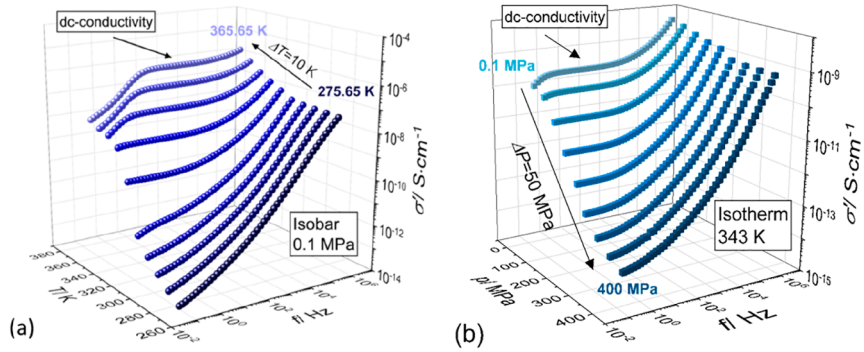

Figure 1. Real part of the complex conductivity of ACB-HCl recorded during isobaric cooling at ambient pressure (a) and isothermal compression at 343 K (b).

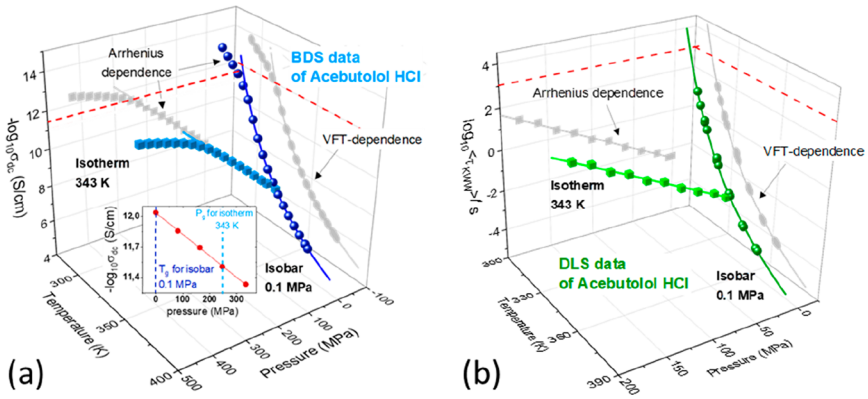

Figure 2. Representative isothermal and isobaric dielectric (a) and DLS (b) data of ACB-HCl in a three-dimensional thermodynamic space and two-dimensional projections (gray symbols). Isobaric experimental data were parametrized by means of the Vogel−Fulcher−Tamman (VFT) equation (above T_g) while isotherms were interpolated by means of the Arrhenius law. Dashed red lines indicate the value of dc-conductivity and structural relaxation at the liquid−glass transition.

isothermal compression are displayed in the 3D plane in Figure 1. Regardless of the thermodynamic path being applied, there are three characteristic dispersive regions of $\sigma'(f)$: (i) a sharp decrease visible in the high-frequency region, (ii) a plateau defining dc-conductivity (σ_{dc}), and (iii) a gradual dropping of the conductivity at the lower frequencies commonly known as the electrode blocking effect.[30] As is clearly visible, the contribution of dc-conductivity to the $\sigma'(f)$ spectra significantly decreases with cooling and squeezing which is due to a dramatic decrease of ion mobility in the vicinity of the liquid−glass transition. The values of $\sigma_{dc}(T, P)$ determined directly from the plateau on $\sigma'(f)$ spectra are presented in Figure 2a. When an isobaric dependence of dc-conductivity is considered, a clear crossover from the super-Arrhenius (Vogel−Fulcher−Tamman-like)[31−33] to Arrhenius-type behavior is visible at a certain temperature (T^{cross} = 314 K). Note that T^{cross} perfectly matches with the calorimetric T_g of ACB-HCl (T_g^{TMDSC} = 315 K). From Figure 2a, it is also obvious that the value of $\log_{10}\sigma_{dc}(T_g)$ is equal to −12 which corresponds to the time scale of charge transport of 0.17 s. This is about three decades above the values characterizing ion transport in classical aprotic ionic liquids (AILs) ($\sigma_{dc}(T_g) = 10^{-15}$ S/cm or $\tau_\sigma = 10^3$ s).[34] At the same time, $\langle\tau_{KWW}\rangle(T_g)$, determined from the DLS experiment, being an equivalent of structural relaxation time τ_α, reaches 10^3 s at T_g (see Figure 2b). This confirms that the charge transport of ACB-HCl is significantly faster than structural reorientation in the vicinity of the liquid−glass transition ($R_\sigma(T_g) = 3$). Specifically, the charge diffusion is continued when the rotational motions of the ACB molecules are already frozen. Importantly, a similar picture appears at high-pressure conditions. Namely, each isotherm reveals a change from one Arrhenius-like behavior to another. The crossover point always occurs at an isochronal structural relaxation time (data not shown). Nevertheless, σ_{dc} determined at the liquid−glass transition continuously increases with pressure (see inset to Figure 2a), thereby indicating a higher contribution of Grotthuss-type conduction to the charge transport in densified ACB-HCl. However, in comparison to other protic ionic glass-formers, the decoupling degree in the studied hydrochloride salt does not change much at elevated pressure, which suggests rather insignificant fluctuations of the H-bonded network in densified material. The physical parameter quantifying this effect is the $d\log_{10}R_\sigma/dP$ coefficient defined as the derivative of $\log_{10}\sigma_{dc}(P_g)/P$ dependence. For ACB-HCl, it is equal to 1.27 GPa^{-1} and indicates that a pressure of 1.27 GPa causes an increase of dc-conductivity by one decade. It is much lower than $d\log_{10}R_\sigma/dP$ reported for low-molecular PI glass-formers;[35] however, at the same time, it is comparable to a pressure coefficient of R_σ found for protic polymerized ionic liquids.[36] In the context of a different efficiency of H^+ hopping in ACB-HCl at ambient and elevated pressures, searching for a new parameter quantifying proton transport over the entire $T-P$ space is fully justified. To verify the suitability of exponent γ for this purpose, we examine the density scaling concept for supercooled and glassy ACB-HCl.

https://dx.doi.org/10.1021/acs.jpcc.0c03548
J. Phys. Chem. C 2020, 124, 15749−15756

To test the scaling behavior of dynamic data of ACB-HCl, the σ_{dc} and $\langle\tau_{KWW}\rangle$ measured at various $T-P$ conditions need to be expressed as a function of volume. For this purpose, the pressure−volume−temperature (PVT) relation for ACB-HCl was additionally determined. The obtained set of $V(T, P)$ data is displayed in the 3D plot in Figure 3. A standard picture

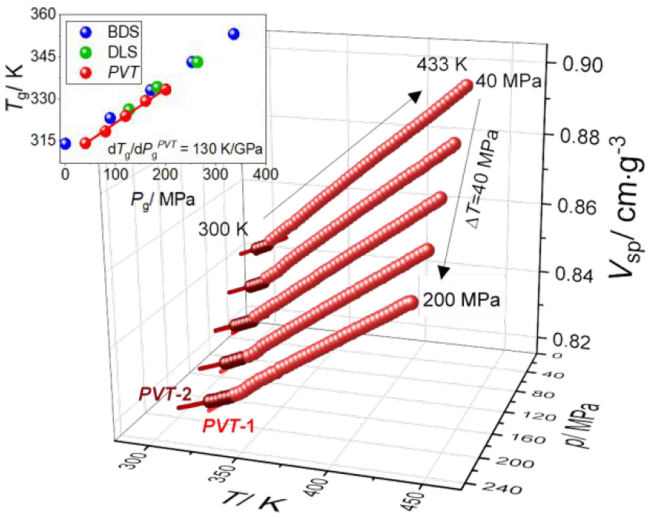

Figure 3. PVT data of ACB-HCl registered above and below T_g (symbols) and parametrized by means of the equation of state (EOS) (lines). Inset panel presents the $T_g(P_g)$ dependence determined from the dielectric, DLS, and PVT measurements.

presenting a decrease of V with cooling and squeezing is observed. Additionally, each collected $V(T, P)$ curve shows crossover behavior, similar to that previously recorded for $\sigma_{dc}(T, P)$ data and denoting a transition from a supercooled to a glassy state. It is noteworthy that the $T_g(P_g)$ behavior taken directly from the crossover of isobaric $V(T)$ data is in good agreement with the $T_g(P_g)$ line constructed from crossover points of $\sigma_{dc}(T, P)$ dependences as well as $T_g(P_g)$ determined from $\langle\tau_{KWW}\rangle$ data by using the isochronal definition of T_g ($T_g = T(\log_{10}\langle\tau_{KWW}\rangle = 3)$) (see inset to Figure 3). This result strongly confirms that the data obtained in three different experiments are consistent with each other.

To calculate the volume at each $T-P$ state point of ACB-HCl, $V(T, P)$ data were parametrized by the means of the equation of state (EOS)[37]

$$V = \frac{A_0 + A_1 \times (T - T_r) + A_2 \times (T - T_r)^2}{\{1 + (\gamma_{EOS}/b_1) \times (P - P_r) \times \exp[b_2 \times (T - T_r)]\}^{1/\gamma_{EOS}}} \quad (1)$$

where A_0, A_1, A_2, γ_{EOS}, b_1, and b_2 are adjustable coefficients shown in Table 1 when T_r = 300 K and P_r = 0.1 MPa. Note that two sets of EOS parameters (PVT-1 and PVT-2) were used to describe $V(T, P)$ data in the supercooled and glassy states of ACB-HCl. Having this, it is now possible to plot the dc-conductivity data and structural relaxation times measured at various T and P as a function of volume. In Figure 4a, very peculiar behavior can be observed for isobaric $\sigma_{dc}(V)$ dependence; i.e., in contrast to $\sigma_{dc}(T^{-1})^{P=0.1}$ there is no crossover from the VFT to the Arrhenius behavior (see 2D projection). Thus, the liquid−glass transition of ACB-HCl becomes hidden when the changes of σ_{dc} accompanying densification at P = const are analyzed. This suggests temperature rather than free volume as a decisive factor in controlling the dynamics of the studied ACB-HCl. A similar result was obtained recently for other protic ionic glass-formers with efficient Grotthuss transports.[38]

The next step toward verification of the scaling criterion in ACB-HCl is to determine the γ exponent. According to the literature reports, there are several approaches to realize this goal. The simplest one is based on the analysis of volume dependences of isobaric and isothermal data (τ_α, η, σ_{dc}) along with the iso(x) lines (x, relaxation time, viscosity, conductivity) in terms of $\log_{10} T = f(\log_{10}V^{-1})$. Namely, $\gamma = d\log_{10}T^{Isox}/d\log_{10}(V^{-1})^{Isox}$. The exemplary horizontal surfaces intersecting the experimental curves at various isoconductivity and isochronous conditions for ACB-HCl are presented in Figure 4a, b, respectively. The insets, in turn, show double logarithmic plots of T vs. V^{-1} obtained along the chosen 2D planes. As presented, $\log_{10}T(\log V^{-1})$ dependences obtained using glassy (G) and supercooled (SL) $\sigma_{dc}(T, V)$ points as well as $\langle\tau_{KWW}\rangle(T, V)$ data are linear. Nevertheless, their slope, providing a direct estimate of the γ parameter, is different in all these cases. Specifically, γ_σ(SL) = 1.86 ± 0.03, and γ_σ(G) = 1.81 ± 0.03, while γ_α(SL) = 2.09 ± 0.05. Importantly, the same coefficients are obtained from an alternative method employing numerical fitting of BDS and DLS data with the use of the Avramov entropic model[39] $\sigma_{dc}(\text{or } \tau_\alpha) = \sigma_0(\text{or } \tau_0)\exp\left(\frac{A}{TV^\gamma}\right)^D$ (see the lines in Figure 4 and Table 2 for fitting parameters: σ_0(or τ_0), γ, A, and D).

Having the values of γ already determined, one can verify the scaling concept for ACB-HCl. As presented in Figure 5, all isothermal and isobaric $\langle\tau_{KWW}\rangle$ dependencies illustrating the structural dynamics of supercooled ACB-HCl create a single curve when plotted as a function of scaling variable $T^{-1}V^{-2.09}$. On the other hand, the $T-P$ dc-conductivity data form two separate master curves for supercooled and glassy regimes, respectively. Thus, the density scaling concept is obeyed for ACB-HCl in each formalism; however, the value of exponent γ is T_g-sensitive and depends on the physical variable being chosen to express the ion dynamics. When the structural relaxation is investigated, the scaling coefficient γ_α of ACB-HCl is similar to the exponents characterizing aprotic ionic liquids (e.g., 1-octyl-3-methylimidazolium tetrafluoroborate [C_8MIM][BF_4] γ_σ = 2.25; 1-hexyl-3-methylimidazolium bis-(trifluoromethylsulfonyl)imide [C_6MIM][NTf_2] γ_η = 2.45)[16] and protic salts (verapamil HCl γ_σ = 2.45[40]), all with "vehicle" transport being decisive. Thus, by exploring solely the diffusion of cations and anions (structural relaxation, viscosity) in terms of the scaling concept, it is not possible to identify the

Table 1. Coefficients of the EOS Equation (eq 1) along with Standard Deviations

	A_0/cm^3 g^{-1}	$A_1 10^4$/cm^3 g^{-1} K^{-1}	$A_2 10^8$/cm^3 g^{-1} K^{-2}	γ_{EOS}	b_1/MPa	$b_2 10^3$/ K^{-1}
PVT-1[a]	0.8525 ± 0.0001	4.51 ± 0.02	−2.39 ± 0.98	11.3 ± 0.1	3084.2 ± 16.0	3.11 ± 0.04
PVT-2[b]	0.8527 ± 0.0001	2.26 ± 0.12	72.8 ± 7.4	15.1 ± 0.8	3416 ± 34	2.76 ± 0.02

[a]Supercooled liquid state. [b]Glass.

https://dx.doi.org/10.1021/acs.jpcc.0c03548
J. Phys. Chem. C 2020, 124, 15749−15756

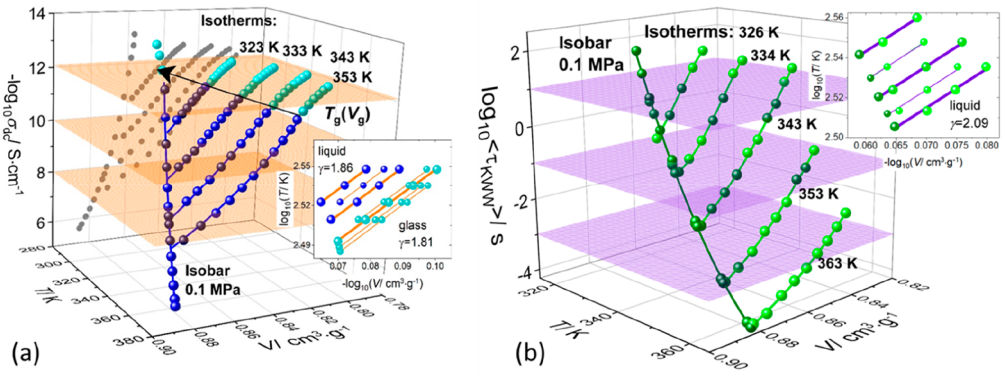

Figure 4. Isothermal and isobaric dependencies of dc-conductivity (a) and structural relaxation times (b) presented as a function of volume. Solid lines denote fits of the Avramov model to the experimental data with the fitting parameters collected in Table 2. Insets present data obtained by horizontal crossing of $\log_{10}\sigma_{dc}(T, V)$ (a) and $\log_{10}\langle\tau_{KWW}\rangle(T, V)$ (b) data at multiple isochronal conditions. Gray symbols in panel (a) present two-dimensional projections of dc-conductivity data.

Table 2. Parameters Obtained from Surface Fitting of Avramov Model to $-\log_{10}\sigma_0$(or τ_0) (T, V) (BDS) and $\log_{10}\langle\tau_{KWW}\rangle(T, V)$ (DLS) Experimental Data

function	param	BDS data	DLS data
Avramov model	$\log_{10}\sigma_0$	2.290	−7.742
	A	388.95	356.45
	D	4.57	5.31
	γ	1.8	2.0

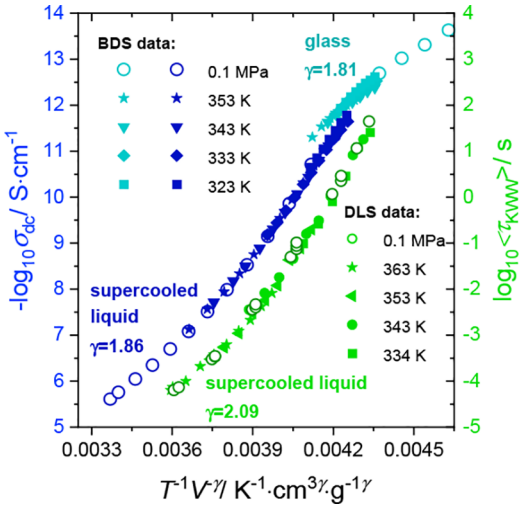

Figure 5. Density scaling curves constructed from dc-conductivity and DLS data of ACB-HCl.

transport mechanism being decisive in a given system. On the other hand, the γ_σ describing the dc-conductivity behavior over a broad $T-P$ space seems to be sensitive to the type of charge carriers taking part in the conduction process, namely, the larger the contribution of proton hopping to overall conductivity (i.e., the larger decoupling between charge transport and ions diffusion), the lower the value of γ_σ. For ACB-HCl, the decrease of 13% is observed from γ_α to γ_σ. Additionally, γ_σ is even lower in the glassy state, when the diffusion of ions gets frozen and protons are the only mobile charge carriers. Generally, this is the second time when the scaling exponent $\gamma_\sigma < 2$ is reported for the protic ionic system. The parameter γ_σ(SL) = 1.12 was obtained for carvedilol dihydrogen phosphate,[38] a material with efficient proton conductivity and decoupling even more pronounced than they are for ACB-HCl. In the context of the presented results, the ratio $\gamma_\sigma/\gamma_\alpha$ can be indeed treated as a new measure of the decoupling phenomenon and, thus, the efficiency of proton transport in supercooled ionic glass-formers over a broad $T-P$ thermodynamic space. An important question arises immediately: Is the relation between scaling exponent and thermodynamic variables established in ref 41 for van der Waals liquids also valid in the case of PI glass-formers?

Following this issue, we verify the formula that links the parameter γ with thermodynamic Grüneisen constant γ_G

$$\gamma = \gamma_{EOS}/D + \gamma_G \tag{2}$$

As mentioned above, the γ_{EOS} is determined directly from PVT data and characterizes the repulsive part of the intermolecular potential. For ACB-HCl, it is equal to 11.3 in supercooled liquid state. On the other hand, parameter D is obtained from the fitting of the experimental $T-V$ surface by means of the Avramov entropic model. Since we have collected two sets of dynamic data for ACB-HCl, describing the behavior of dc-conductivity and structural relaxation over a wide $T-V$ space, we have two different γ coefficients and two different parameters D. Nevertheless, by using both these data sets, a nonphysical Grüneisen constant is obtained. This is because the ratio γ_{EOS}/D is larger than the scaling parameter γ (see Table 3). Interestingly, in the past, the validity of eq 2 was confirmed for several van der Waals liquids and aprotic ionic system 1-butyl-1-methylpyrrolidinium bis(oxalate)borate [C_4MPYR][BOB] species.[41] However, in all these cases the value of γ was around 4, i.e., 2 times higher than the coefficients determined for ACB-HCl. Importantly, the negative value of γ_G is obtained also for other protic ionic glass-formers, i.e., hydrochloride salts of lidocaine, carvedilol, as well as carvedilol H_2PO_4 (see Table 3 for γ_{EOS}, D, and γ_G). This indicates that eq 2 is broken for PI materials. In this context, it is interesting to calculate the real Grüneisen constant for protic conductors. For this purpose, we determine γ_G directly from the thermodynamic variables:[42]

$$\gamma_G = \frac{V\alpha_P}{C_V\kappa_T} \tag{3}$$

where V is a specific volume, α_P the isobaric thermal expansion coefficient, and κ_T the isothermal compressibility. The C_V is the heat capacity at a constant volume that can be converted to the

https://dx.doi.org/10.1021/acs.jpcc.0c03548
J. Phys. Chem. C 2020, 124, 15749−15756

Table 3. Dynamic and Thermodynamic Parameters of Selected Protic Ionic Glass-Formers

	ACB-HCl	carvedilol HCl	carvedilol H_2PO_4	lidocaine HCl
γ	1.8[a]	2.13[a]	1.12[a]	2.40[a]
	2.0[b]			
γ_{EOS}	11.3	11.92	9.83	10.48
D	4.57[a]	4.95[a]	4.95[a]	3.05[a]
	5.31[b]			
γ_{EOS}/D	2.47[a]	2.40[a]	1.98[a]	3.43[a]
	2.128[b]			
$\gamma_G(T_g)$ (eq 3)	0.64	0.81	0.74	0.86[d]
C_P/J g^{-1} K^{-1} (T_g)	2.15	2.00	1.99[c]	NA
$\alpha_P 10^4$/K (T_g)	5.183	5.592	5.559	NA
$\kappa_T 10^4$/ MPa (T_g)	3.345	3.126	3.045	NA
V/cm^3 g^{-1}	0.8585	0.7998	0.8036	NA

[a]Determined from BDS data. [b]Determined from DLS data. [c]Estimated using group contribution method.[47] [d]Taken from ref 48.

heat capacity at constant pressure C_P that, in turn, is easily available in DSC measurements: $C_V = C_P - \frac{TV\alpha_P^2}{\kappa_T}$. Since all the thermodynamic quantities defining γ_G depend on T−P conditions, the common practice is to define the Grüneisen constant at the liquid−glass transition of the given system. Having already determined all the quantities appearing in eq 3 (see Table 3), we calculated the value of the exponent $\gamma_G(T_g)$ = 0.64 for ACB-HCl. Interestingly, the $\gamma_G(T_g)$ value below unity is found also for other protic materials (see Table 3). On the other hand, the obtained values are around twice lower than $\gamma_G(T_g)$ for classical aprotic ionic liquids $1.1 < \gamma_G(T_g) < 1.5$ (e.g., 1-butyl-3-methylimidazolium bis-(pertrifluoroethylsulfonyl)imide [C_4MIM][BETI] = 1.3; [C_4MPYR][BOB] = 1.5; 1-butyl-3-methylimidazolium bis-(trifluoromethylsulfonyl)imide [C_4MIM][NTf_2] = 1.32),[43,44] and the van der Waals systems (e.g., BMPC = 2.26; OTP = 1.2).[45] Such a low value of $\gamma_G(T_g)$ found for ACB-HCl and other protic glass-formers is most likely due to their relatively high isobaric heat capacity since the other parameters (V_m, α_P, and κ_T) stay typical for AILs. Since the molar heat capacity generally increases linearly with the molar mass and molar volume of the IL,[46] one can expect that the high C_P of protic materials studied herein is due to their heavy cations containing more bonds storing thermal energy and having more degrees of freedom than the classical cations of ILs, i.e., imidazolium or pyrrolidinium-based. The proton transport between cations and anions is of rather less importance.

CONCLUSIONS

In this paper, we have investigated the molecular dynamics of the ACB-HCl protic ionic glass-former with efficient inter- and intramolecular proton transport. Due to the contribution of Grotthuss conduction, the charge transport of ACB-HCl is markedly faster than the structural relaxation, especially in the vicinity of the liquid−glass transition and under high-pressure conditions. To quantify the effectiveness of H^+ hopping over a wide T−P range, we took advantage of the density scaling concept. We found that TV^{γ} scaling is satisfied for ACB-HCl despite the significant contribution of H-bonding to intermolecular interactions. However, the exponent γ depends on the dynamic quantity under investigation. The γ_σ (obtained from scaling of $\sigma_{dc}(T, P)$ data) in contrast to γ_α (from analysis of structural dynamics) is sensitive to the type of charge carrier participating in the conduction process; i.e., it decreases when the efficiency of H^+ hopping is higher, and generally it is ≈2 times smaller than γ_σ of AILs. Consequently, the ratio $\gamma_\sigma/\gamma_\alpha$ can be considered as a new measure of decoupling between charge and mass transport in protic ionic systems, and thereby the contribution of the Grotthuss mechanism to overall conductivity at various T−P state points. At the same time, the proton dynamics is not detectable by revising the thermodynamic quantities characterizing a given system. The Grüneisen constant γ_G of protic ionic glass-formers, although markedly lower than γ_G reported for AILs, reflects the complex structure of the cation rather than H-bonding interactions and H hopping.

AUTHOR INFORMATION

Corresponding Author

Zaneta Wojnarowska − *Institute of Physics, University of Silesia in Katowice, SMCEBI, Chorzow 41-500, Poland;* orcid.org/0000-0002-7790-2999; Email: Zaneta.wojnarowska@smcebi.edu.pl

Authors

Małgorzata Musiał − *Institute of Physics, University of Silesia in Katowice, SMCEBI, Chorzow 41-500, Poland;* orcid.org/0000-0002-1624-6617

Shinian Cheng − *Institute of Physics, University of Silesia in Katowice, SMCEBI, Chorzow 41-500, Poland;* orcid.org/0000-0002-5615-8646

Jacek Gapinski − *Faculty of Physics, A. Mickiewicz University, 61-614 Poznań, Poland;* orcid.org/0000-0001-6356-6608

Adam Patkowski − *Faculty of Physics, A. Mickiewicz University, 61-614 Poznań, Poland*

Jürgen Pionteck − *Leibniz Institute of Polymer Research Dresden, D-01069 Dresden, Germany;* orcid.org/0000-0003-2310-1106

Marian Paluch − *Institute of Physics, University of Silesia in Katowice, SMCEBI, Chorzow 41-500, Poland;* orcid.org/0000-0002-7280-8557

Complete contact information is available at: https://pubs.acs.org/10.1021/acs.jpcc.0c03548

Author Contributions

The manuscript was written through contributions of all authors. All authors have given approval to the final version of the manuscript.

Notes

The authors declare no competing financial interest.

ACKNOWLEDGMENTS

The authors are deeply grateful for the financial support by the National Science Centre within the framework of the Opus15 project (Grant DEC- 2018/29/B/ST3/00889).

REFERENCES

(1) Acharya, R.; Carnevale, V.; Fiorin, G.; Levine, B. G.; Polishchuk, A. L.; Balannik, V.; Samish, I.; Lamb, R. A.; Pinto, L. H.; DeGrado, W. F.; et al. Structure and mechanism of proton transport through the transmembrane tetrameric M2 protein bundle of the influenza A virus. *Proc. Natl. Acad. Sci. U. S. A.* **2010**, *107*, 15075−15080.

(2) Zeng, Y.; Li, A.; Yan, T. Hydrogen Bond Dynamics in the Solvation Shell on Proton Transfer in Aqueous Solution. *J. Phys. Chem. B* **2020**, *124*, 1817−1823.

(3) Kornyshev, A. A.; Kuznetsov, A. M.; Spohr, E.; Ulstrup, J. Kinetics of proton transport in water. *J. Phys. Chem. B* **2003**, *107*, 3351−3366.
(4) Kreuer, K.-D. Proton Conductivity: Materials and Applications. *Chem. Mater.* **1996**, *8*, 610−641.
(5) Armand, M.; Endres, F.; MacFarlane, D. R.; Ohno, H.; Scrosati, B. Ionic-liquid materials for the electrochemical challenges of the future. *Nat. Mater.* **2009**, *8*, 621−629.
(6) Fumino, K.; Wulf, A.; Ludwig, R. The potential role of hydrogen bonding in aprotic and protic ionic liquids. *Phys. Chem. Chem. Phys.* **2009**, *11*, 8790−4.
(7) Angell, C. A.; Xu, W.; Yoshizawa, M.; Hayashi, A.; Belieres, J.-P.; Lucas, P.; Videa, M. Physical chemistry of ionic liquids, inorganic and organic, protic and aprotic. *Chemistry of Ionic Liquids*; Ohno, H., Ed.; Wiley: New York, 2005; pp 5−23.
(8) Greaves, T. L.; Drummond, C. J. Protic ionic liquids: properties and applications. *Chem. Rev.* **2008**, *108*, 206−237.
(9) Yoshizawa, M.; Xu, W.; Angell, C. A. Ionic liquids by proton transfer: vapor pressure, conductivity, and the relevance of _pKa from aqueous solutions. *J. Am. Chem. Soc.* **2003**, *125*, 15411.
(10) Vilciauskas, L.; Tuckerman, M. E.; Bester, G.; Paddison, S. J.; Kreuer, K.-D. The mechanism of proton conduction in phosphoric acid. *Nat. Chem.* **2012**, *4*, 461−466.
(11) Stoimenovski, J.; Izgorodina, E. I.; MacFarlane, D. R. Ionicity and proton transfer in protic ionic liquids. *Phys. Chem. Chem. Phys.* **2010**, *12*, 10341−7.
(12) Wojnarowska, Z.; Wang, Y.; Paluch, K. J.; Sokolov, A. P.; Paluch, M. Observation of highly decoupled conductivity in protic ionic conductors. *Phys. Chem. Chem. Phys.* **2014**, *16*, 9123.
(13) Ingram, M. D. Ionic conductivity and glass structure. *Philos. Mag. B* **1989**, *60*, 729−740.
(14) Wojnarowska, Z.; Wang, Y.; Pionteck, J.; Grzybowska, K.; Sokolov, A. P.; Paluch, M. High Pressure as a Key Factor to Identify the Conductivity Mechanism in Protic Ionic Liquids. *Phys. Rev. Lett.* **2013**, *111*, 225703.
(15) Wojnarowska, Z.; Paluch, K. J.; Shoifet, E.; Schick, C.; Tajber, L.; Knapik, J.; Wlodarczyk, P.; Grzybowska, K.; Hensel-Bielowka, S.; Verevkin, S. P.; et al. Molecular origin of enhanced proton conductivity in anhydrous ionic systems. *J. Am. Chem. Soc.* **2015**, *137*, 1157−1164.
(16) Paluch, M. *Dielectric Properties of Ionic Liquids*; Springer: Berlin, 2016.
(17) Gundermann, D.; Pedersen, U. R.; Hecksher, T.; Bailey, N. P.; Jakobsen, B.; Christensen, T.; Olsen, N. B.; Schrøder, T. B.; Fragiadakis, D.; Casalini, R.; et al. Predicting the density-scaling exponent of a glass-forming liquid from Prigogine−Defay ratio measurements. *Nat. Phys.* **2011**, *7*, 816−821.
(18) Hoover, W. G.; Rossj, M. Statistical theories of melting. *Contemp. Phys.* **1971**, *12*, 339−356.
(19) Floudas, G.; Paluch, M.; Grzybowski, A.; Ngai, K. *Molecular Dynamics of Glass-Forming Systems: Effects of Pressure*; Advances in Dielectrics; Springer-Verlag: Berlin, 2011.
(20) López, E. R.; Pensado, A. S.; Comuñas, M. J.; Pádua, A. A.; Fernández, J.; Harris, K. R. Density scaling of the transport properties of molecular and ionic liquids. *J. Chem. Phys.* **2011**, *134* (14), 144507.
(21) Wojnarowska, Z.; Jarosz, G.; Grzybowski, A.; Pionteck, J.; Jacquemin, J.; Paluch, M. On the scaling behavior of electric conductivity in $[C_4mim][NTf_2]$. *Phys. Chem. Chem. Phys.* **2014**, *16*, 20444.
(22) López, E. R.; Pensado, A. S.; Fernández, J.; Harris, K. R. On the density scaling of pVT data and transport properties for molecular and ionic liquids. *J. Chem. Phys.* **2012**, *136*, 214502.
(23) Wojnarowska, Z.; Musiał, M.; Dzida, M.; Paluch, M. Experimental Evidence for a State-Point-Independent Density-Scaling Exponent in Ionic Liquids. *Phys. Rev. Lett.* **2019**, *123*, 125702.
(24) Pensado, A. S.; Pádua, A. A. H.; Comuñas, M. J. P.; Fernández, J. Relationship between Viscosity Coefficients and Volumetric Properties Using a Scaling Concept for Molecular and Ionic Liquids. *J. Phys. Chem. B* **2008**, *112*, 5563−5574.
(25) Pochylski, M.; Gapiński, J.; Wojnarowska, Z.; Paluch, M.; Patkowski, A. Nature of intramolecular dynamics in protic ionic glass-former: insight from ambient and high pressure Brillouin spectroscopy. *J. Mol. Liq.* **2019**, *282*, 51−56.
(26) Wojnarowska, Z.; Rams-Baron, M.; Knapik-Kowalczuk, J.; Połatyńska, S.; Pochylski, M.; Gapinski, J.; Patkowski, A.; Wlodarczyk, P.; Paluch, M. Experimental evidence of high pressure decoupling between charge transport and structural dynamics in a protic ionic glass-former. *Sci. Rep.* **2017**, *7* (1), 7084.
(27) GNOMIX INC.: Boulder, CO.
(28) Fakhreddin, Y. A.; Zoller, P. *Society of Plastic Engineers ANTEC'91* **1991**, *36*, 1642.
(29) Zoller, P.; Walsh, D. *Standard Pressure−Vol.−Temperature Data for Polymers*; Technomic: Lancaster, PA, 1995.
(30) Kremer, A. S. *Broadband Dielectric Spectroscopy*; Springer, 2003.
(31) Vogel, H. The law of the relation between the viscosity of liquids and the temperature. *Physikalische Zeitschrift* **1921**, *22*, 645−646.
(32) Fulcher, G. Analysis of recent measurements of the viscosity of glasses. *J. Am. Ceram. Soc.* **1925**, *8*, 339−355.
(33) Tammann, G.; Hesse, W. Die Abhängigkeit der Viscosität von der Temperatur bie unterkühlten Flüssigkeiten. *Zeitschrift für anorganische und allgemeine Chemie* **1926**, *156* (1), 245−257.
(34) Mizuno, F.; et al. Highly decoupled ionic and protonic solid electrolyte systems, in relation to other relaxing systems and their energy landscapes. *J. Non-Cryst. Solids* **2006**, *352*, 5147−5155.
(35) Wojnarowska, Z.; Paluch, M. Recent progress in dielectric properties of protic ionic liquids. *J. Phys.: Condens. Matter* **2015**, *27*, 073202.
(36) Wojnarowska, Z.; Feng, H.; Diaz, M.; Ortiz, A.; Ortiz, I.; Knapik-Kowalczuk, J.; Vilas, M.; Verdía, P.; Tojo, E.; Saito, T.; Stacy, E. W.; Kang, N.-G.; Mays, J. W.; Kruk, D.; Wlodarczyk, P.; Sokolov, A. P.; Bocharova, V.; Paluch, M. Revealing the charge transport mechanism in polymerized ionic liquids: Insight from high pressure conductivity studies. *Chem. Mater.* **2017**, *29*, 8082−8092.
(37) Grzybowski, A.; Grzybowska, K.; Paluch, M.; Swiety, A.; Koperwas, K. Density scaling in viscous systems near the glass transition. *Phys. Rev. E* **2011**, *83* (4), 041505.
(38) Wojnarowska, Z.; Tajber, L.; Paluch, M. Density Scaling in Ionic Glass Formers Controlled by Grotthuss Conduction. *J. Phys. Chem. B* **2019**, *123*, 1156−1160.
(39) Casalini, R.; Mohanty, U.; Roland, C. M. Thermodynamic interpretation of the scaling of the dynamics of supercooled liquids. *J. Chem. Phys.* **2006**, *125*, No. 014505.
(40) Wojnarowska, Z.; Paluch, M.; Grzybowski, A.; Adrjanowicz, K.; Grzybowska, K.; Kaminski, K.; Wlodarczyk, P.; Pionteck, J. Study of molecular dynamics of pharmaceutically important protic ionic liquid-verapamil hydrochloride: I.Test of thermodynamic scaling. *J. Chem. Phys.* **2009**, *131*, 104505.
(41) Paluch, M.; Haracz, S.; Grzybowski, A.; Mierzwa, M.; Pionteck, J.; Rivera-Calzada, A.; Leon, C. A relationship between Intermolecular potential, thermodynamics, and dynamic scaling for a supercooled ionic liquid. *J. Phys. Chem. Lett.* **2010**, *1*, 987−92.
(42) Hartwig, G. *Polymer Properties at Room and Cryogenic Temperatures: Thermal Expansion and the Grueneisen Relation New York*; Plenum Press: New York, 1994; Chapter 4.
(43) Paluch, M.; Haracz, S.; Grzybowski, A.; Mierzwa, M.; Pionteck, J.; Rivera-Calzada, A.; Leon, C. Relationship between Intermolecular Potential, Thermodynamics, and Dynamic Scaling for a Supercooled Ionic Liquid. *J. Phys. Chem. Lett.* **2010**, *1* (6), 987−992.
(44) Cheng, S.; Musiał, M.; Wojnarowska, Z.; Holt, A.; Roland, C. M.; Drockenmuller, E.; Paluch, M. Structurally Related Scaling Behavior in Ionic Systems. *J. Phys. Chem. B* **2020**, *124* (7), 1240−1244.
(45) Roland, C. M.; Casalini, R. Entropy basis for the thermodynamic scaling of the dynamics of o-terphenyl. *J. Phys.: Condens. Matter* **2007**, *19*, 205118.

https://dx.doi.org/10.1021/acs.jpcc.0c03548
J. Phys. Chem. C 2020, 124, 15749−15756

(46) MacFarlane, D. R.; Kar, M.; Pringle, J. M. *Fundamentals of Ionic Liquids: From Chemistry to Applications*; Wiley-VCH Verlag GmbH & Co. KGaA, 2017.
(47) Oster, K.; Jacquemin, J.; Hardacre, C.; Ribeiro, A. P. C.; Elsinawi, A. Further Development of the Predictive Models for Physical Properties of Pure Ionic Liquids: Thermal Conductivity and Heat Capacity. *J. Chem. Thermodyn.* **2018**, *118*, 1−5.
(48) Wojnarowska, Z.; Roland, C. M.; Kolodziejczyk, K.; Swiety-Pospiech, A.; Grzybowska, K.; Paluch, M. Quantifying the Structural Dynamics of Pharmaceuticals in the Glassy State. *J. Phys. Chem. Lett.* **2012**, *3*, 1238.

https://dx.doi.org/10.1021/acs.jpcc.0c03548
J. Phys. Chem. C 2020, 124, 15749−15756